

# Assessment of Empirical Formulas for Estimating Residual Axial Capacity of Blast Damaged RC Columns

By Mohammad Esmailnia Omran<sup>1</sup>, Somayeh Mollaei<sup>2</sup>

## Abstract

Columns are the most important load bearing structural elements in buildings. Under the effect of external explosions near the building, columns in the ground and first floors may have severe damage that can cause progressive collapse of the whole building frames. Residual axial load bearing capacity of the reinforced concrete column after the effect of lateral blast loading could be a practical criterion to damage assessment of the column. This is essential to determine whether the column has to be replaced or repaired for future use. In this paper, residual axial capacity of the square RC columns under the effect of initial axial force and lateral blast loading is investigated. Explicit finite element package LS-DYNA is used for analysis of the considered models and determining their residual capacity. There are some empirical formulas for estimating of the residual axial capacity of the blast damaged RC columns including Bao and Li (2010), Wu et al (2010) and Arlery et al (2013). Here, FEM results are compared to the estimations of these formulas. Different levels of initial axial force in the columns and different scale distances of blast loading are considered.

*Keywords: blast loading, reinforced concrete column, residual axial capacity, LS-DYNA.*

## 1. Introduction

Columns are one of the most critical structural elements in the buildings and other frame structures. Under intentional or accidental explosions near the building external columns are the most vulnerable structural elements. Severe damage to a column may cause its failure and elimination of the load bearing system. This could be followed by progressive collapse of the whole building or some part of that. Hence, investigation of the dynamic behavior and axial load bearing capacity of the RC columns under blast loading is a very important concept. Estimation of residual axial capacity of the column is essential to determine whether the column has to be replaced or repaired for future use.

As a criterion for defining the intensity of the damage sustained by the column under blast loading, damage index  $D$  has been introduced by equation 1 [1,2]. The value of  $D=1$  corresponds to complete failure of the column and  $D=0$  shows that there is not important damage in the column.

$$D=1-\frac{P_r}{P_{max}} \quad (1)$$

At the above equation,  $P_r$  is residual axial load capacity of the blast damaged column and  $P_{max}$  is the nominal pure axial strength of the column before blast loading. If  $0 \leq D \leq 0.2$  damage level assessment is low, if  $0.2 < D \leq 0.5$  damage level is medium, if  $0.5 \leq D < 0.8$  damage level degree is high and  $0.8 \leq D \leq 1.0$  corresponds collapse of the column under the blast loading [2]. This damage criterion based on residual axial capacity of the

<sup>1</sup>Assistant professor, Department of Civil Engineering, University of Kurdistan, Sanandaj, Iran

<sup>2</sup>PhD student, Department of Civil Engineering, University of Kurdistan, Sanandaj, Iran

column, despite of other criteria such as maximum displacement and deflection, is independent of the behavior mode of the structure. Some of the researches have been done in this field.

Li et al (2012) experimentally investigated two specimen series (limited seismic and non-seismic) subjected to simulated blast loading and axial force [3]. In this study, hydraulic actuators were installed to reproduce predicted residual lateral deflection under blast loading and to apply the axial load and measure the residual axial capacity of the damaged columns. The effects of parameters such as axial loading and the transverse reinforcement ratio were investigated. The results showed the improved performance that columns detailed with a higher transverse reinforcement ratio have an increased residual axial capacity when laterally damaged. Axial load (service load) on the columns was also found to affect the residual deflection profile and residual axial capacity of the column [3].

Computer software LS-DYNA was utilized by Bao and Li (2010) to provide numerical simulations of the dynamic response and residual axial strength of RC columns subjected to blast loads [4]. In this study, the standoff distance was assumed to be 5 m and various charges weighing between 0 and 1 ton equivalent TNT were used. Blast loading at different points on the front surface of the column was computed by LS-DYNA with the built-in CONWEP blast model. A parametric study was carried out on a series of 12 columns to investigate the effects of transverse reinforcement ratio, axial load ratio, longitudinal reinforcement ratio, and column aspect ratio. These various parameters were incorporated into a proposed formula, capable of estimating the residual axial capacity of the blast damaged column as follows [4]:

$$\nu = \left[ 73.65\rho_v + 8.465\rho_g - 0.020879(L/b) + 0.104 \right] \times e^{\left[ 89284.22\rho_v - 1308.64221\rho_g - 9.684203(L/b) - 382.12 \right] \left( \rho_r/L \right) \left( \frac{P_L}{f_c A_g} \right)} \quad (2)$$

Where,  $\rho_v$  is transverse reinforcement ratio,  $\rho_g$  longitudinal reinforcement ratio,  $L$  clear height of the column,  $b$  width of the section,  $y_r$  residual lateral displacement at mid-height,  $P_L$  initial long term axial force,  $f_c$  concrete characteristic compressive strength and  $A_g$  gross section area of the column. Ratio  $y_r/L$  is defined as behavioral index of the RC column for investigation of its residual axial capacity. Ratio of residual axial strength  $\nu$  is defined by the following equation:

$$\nu = \frac{P_r - P_L}{P_{max} - P_L} \quad (3)$$

When the column is undamaged (before blast loading) we have  $P_r = P_{max}$  and  $\nu = 1$ . When the column has lost the ability to sustain the long-term axial load  $P_r = P_L$  and  $\nu = 0$ . Mostly, ultimate state of the RC column is defined by demolishing axial load carrying capacity of the column [5]. Based on equation 2, residual axial strength is smaller under larger axial load and it increases with an increase in the longitudinal reinforcement ratio. As well, residual axial capacity ratio increases with a reduction in the aspect ratio ( $L/b$ ).

Another relation for near-field blast condition was developed by Wu et al (2010) for

estimation of residual axial strength of the columns [6]. In their study, high-fidelity physics based computer program LS-DYNA was utilized to provide numerical simulations of the dynamic response and residual axial capacity of RC columns subjected to blast loads. In their research, Arbitrary Lagrange-Euler (ALE) approach was used to model the interface between the air and the structure. In the modeling, air was assumed to be an ideal gas and high explosive (TNT) was modeled by using Jones-Wilkins-Lee (JWL) EOS. An extensive parametric study was conducted to investigate the relationship between residual axial capacity and structural and loading parameters such as material strength, column detail and blast conditions. Two empirical equations were derived to predict the residual capacity index of the column. The empirical equation for the case scenario where the TNT explosive is located at the bottom of column is expressed as follows:

$$\frac{P_r}{P_{max}} = \left(0.02\rho_v + 0.05\rho_g - 0.00035\right) \omega_{TNT} \left(15\rho_g^{-10}\rho_v^{-0.5} \frac{P_L}{f_c A_g}^{-1.725}\right) \leq 1.0 \quad (4)$$

The other empirical equation for the case scenario where the TNT explosive is located at a height of 1.5 m from the footing of column is expressed as follows:

$$\frac{P_r}{P_{max}} = 1.1 - \left(-360\rho_v - 300\rho_g - 5 \frac{P_L}{f_c A_g} + 20.7\right) \omega_{TNT} \leq 1.0 \quad (5)$$

In the above equations, non-dimensional column dimension parameter ( $\omega_{TNT}$ ) is defined as the ratio of TNT explosive mass to the mass of a 1 m high concrete column and its value is less than 0.04. According to equations 4 and 5, an increase in column depth results in less  $\omega_{TNT}$  and as such, a column will be able to sustain higher axial loads in its post-blast state. As well, the column height does not affect the blast response. In a column with higher axial load ratio the damage due to blast load is milder. Residual capacity index of blast damaged RC column with low transverse reinforcement ratio is less than that of the column with high transverse reinforcement ratio [6].

Arlery et al (2013) used coupled fluid dynamics and finite element calculations to investigate RC columns response for contact and near-field detonations from 2.5-500 kg of TNT [1]. The explosive charge was supposed to be spherical and blast load was calculated with the Eulerian solver of the OURANOS code. In the numerical model, air was assumed to be an ideal gas and high explosive TNT was modeled with a Mie-Grüneisen equation of state and the Jones-Wilkins-Lee formalism for the reference curve. The dynamic response of the column was calculated with ABAQUS/ Explicit. Then, the residual axial bearing capacity of the blast-damaged column was evaluated with a quasi-static ABAQUS Explicit calculation. Parametric studies were then carried out to investigate the influence of charge weight, stand-off distance, column dimensions and concrete strength. Based on these results, an analytical empirical formula is derived to predict the damage level of the column and its residual axial load-carrying capacity as follow [1]:

$$D = 0.692 + b_{11} + [b_{21} \text{ or } b_{22} \text{ or } b_{23}] + [b_{31} \text{ or } b_{32} \text{ or } b_{33}] + [b_{41} \text{ or } b_{42} \text{ or } b_{43}] + [b_{51} \text{ or } b_{52} \text{ or } b_{53} \text{ or } b_{54}] + [b_{61} \text{ or } b_{62} \text{ or } b_{63} \text{ or } b_{64}] \quad (6)$$

$b_{ij}$  ( $i=1-6$  and  $j = 1, 2, 3$  or  $4$ ) are coefficients related to each of the different effective

parameters which values are given in table 1.

**Table 1:** Parameters of Arlery et al (2013) formula [1].

$\frac{a}{b}$	$\frac{a}{b} = 1$	$b_{11} = -0.007$
	$\frac{a}{b} = 2$	$b_{12} = 0.007$
$\hat{f}_c$ (MPa)	25	$b_{21} = 0.06$
	35	$b_{22} = -0.038$
	50	$b_{23} = -0.022$
L (m)	3.3	$b_{31} = 0.02$
	4.6	$b_{32} = -0.029$
	6.6	$b_{33} = -0.049$
a (m)	0.25	$b_{41} = 0.143$
	0.35	$b_{42} = 0.074$
	0.5	$b_{43} = -0.217$
d (m)	0.07	$b_{51} = -0.313$
	0.11	$b_{52} = 0.109$
	0.15	$b_{53} = 0.089$
	0.25	$b_{54} = 0.175$
R/d	1.25	$b_{61} = 0.103$
	1.6	$b_{62} = 0.095$
	$b_{63} = 0.017$	$b_{63} = 0.017$
	$b_{64} = -0.214$	$b_{64} = -0.214$

In the above table,  $a$  is the depth of the cross section,  $d$  is radius of the spherical explosive and  $R$  is the standoff distance. The choice of each coefficient depends on the value considered for the associated variable. For instance, for an experiment with square column section ( $b=0.25$  m) and  $\hat{f}_c = 25$  Mpa  $\cdot L=6.6$  m,  $d=0.1099$  m and  $R/d=4$ , coefficients  $b_{11}$ ,  $b_{21}$ ,  $b_{33}$ ,  $b_{41}$ ,  $b_{52}$  and  $b_{64}$  have to be chosen.  $D$  finally equals to  $D = 0.692 + b_{11} + b_{21} + b_{33} + b_{41} + b_{52} + b_{64}$ . For values of the parameters which are different from the one defined in table 1,  $D$  can be obtained using linear interpolation or extrapolation of the coefficients  $b_{ij}$ .

Based on the main results obtained by Arlery et al (2013), for the case of close-in and near-field detonations, thickness of the column, the charge radius and the ratio of standoff distance to charge radius proved to be the most significant on the column response. The column width, the column height and the concrete compressive strength do not play an important role [1].

Here, the main target is comparison of the estimated residual axial capacity of the blast damaged RC columns by empirical formulas with explicit finite element analysis results. At first, FE modeling and analysis using LS-DYNA software is described and verified in compare to an experimental explosion test results. Then, the process is used to analysis of RC column models under lateral simultaneous effect of blast loading and axial compressive force. Finally, blast damaged columns are analyzed under axial load to determine their axial strength. Obtained results are compared to the estimations of three empirical equations described above.

## 2. FE Analysis by LS-DYNA

Considered models include 9 RC columns with square cross-sectional dimension of  $350 \times 350$  mm and a vertical height of 3000 mm. Geometry and material details of all models are the same and the only different parameters in the columns is loading scenarios. Characteristic compressive strength of the concrete is assumed to be 35 MPa and yield and ultimate stress of reinforcing bars is 400 and 600 MPa, respectively. Longitudinal reinforcement of four  $\varphi 25$  bars and transverse reinforcement of  $\varphi 10$  placed 200 mm apart. A concrete cover of 50 mm is assumed. All the RC columns are designed as conventional columns in accordance with the ACI 318 code.

The explicit nonlinear FEM program LS-DYNA [7-9] is utilized in this paper for axial and blast loading and analysis of considered RC columns. Geometric and loads modeling process including blast loadings definition, structural geometry and boundary conditions, material models and FE meshing, is done by LS-PrePost [10,11]. This program has a very powerful user-friendly graphic interface for pre-processing (modeling) and post-processing (interpretation of analysis results). Afterward, structural analysis is done using explicit LS-DYNA solver.

When blast wave hits the front face of a structure reflected pressure is instantly developed, and this is the most destructive aspect of blast loading on a structure. Here, the explosion center is assumed at the mid-height of the column. Blast pressure distribution on the front face of the column is computed by built-in Load Blast Enhanced (LBE) model in LS-DYNA based on considered charge weight and standoff distance. LBE relates the reflected overpressure to the scaled distance and also accounts for the angle of incidence of the blast wave [7].

Eight-nod SOLID hexahedron elements with a single integration point with 15 mm size are used to represent concrete. The reinforcing bars are modeled explicitly using two-node Hughes–Liu BEAM elements with 30 mm length connected to the concrete mesh nodes. These connection nodes are not able to slip (perfectly bonded). As a result, there is complete compatibility of strains between concrete and steel elements. Transverse reinforcement elements are defined as BEAM elements to take into account their effects on the confinement of core concrete [7]. The restraints at bottom end of the column is assumed to be ideal fixed support while at the top of the column there is only displacement freedom through axial axis of the column (roller support). A rigid plate which is only allowed to move in the vertical direction is attached to the top end for applying axial pressure. Figure 1 shows the three-dimensional model of the column.

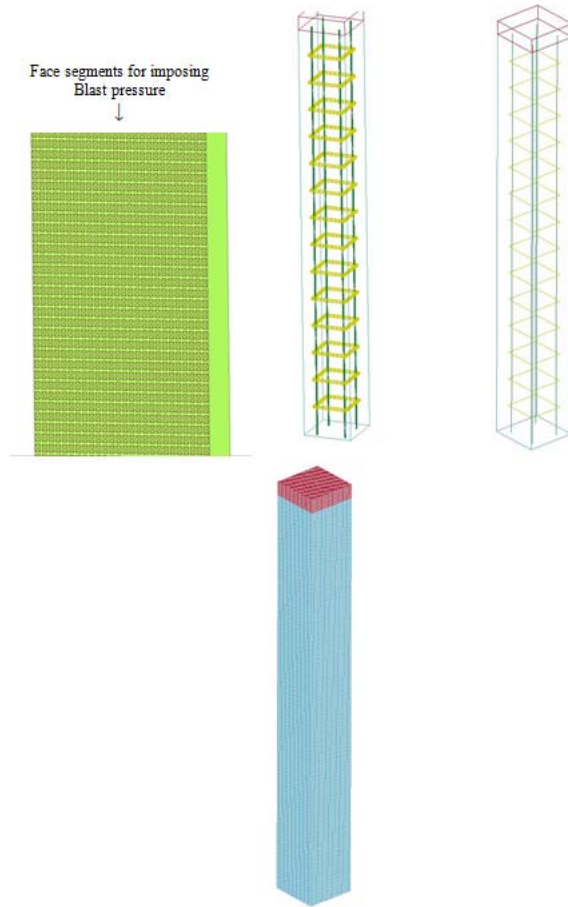


Figure 1: FE model of RC column in LS-DYNA.

In order to control hourglassing event, here type3 option in LS-DYNA is selected under blast loading and type5 is selected under axial loading. Type3 option is based on viscosity and type5 is based on stiffness. When there is high strain rate conditions such as blast loading, using stiffness controls may lead to unrealistic increase in damage level of the elements [12].

## 2.1 Concrete material model

LS-DYNA code contains several material models that can be used to represent concrete under dynamic loading conditions such as material type 5 (soil and crushable foam), type 14 (soil and crushable foam failure), type 16 (pseudo tensor), type 25 (geological cap model), type 72RW3 (concrete damage), type 84 (Winfrith concrete), type 96 (brittle damage), type 111 (Johnson Holmquist Concrete) and type 159 (continuous surface cap model-CSCM) [7-9]. In this paper, material type 72RW3 (MAT\_CONCRETE\_DAMAGE) is used which is the third release of Karagozian and Case (K&C) concrete model. It is a plasticity-based model, using three shear failure

surfaces and including damage and strain rate effects [13,14]. The model has a default parameter generation function based on the unconfined compressive strength of the concrete and provides a robust representation of complex concrete response [13]. In this model, the stress tensor is expressed as the sum of the hydrostatic stress tensor and the deviatoric stress tensor. The hydrostatic tensor changes the concrete volume and the deviatoric stress tensor controls the shape deformation. For the hydrostatic stress tensor, the compaction model is a multi-linear approximation in internal energy. Pressure is defined by equation 7 [8].

$$P=C(\varepsilon_p)+\gamma T(\varepsilon_p)E \tag{7}$$

Where  $E$  is the internal energy per initial volume,  $\gamma$  is the ratio of specific heats. The volumetric strain  $\varepsilon_p$  is given by the natural logarithm of the relative volume and  $C$  and  $T$  are functions of logarithmic the volumetric strain. Under compressive condition  $\varepsilon_p$  is assumed to be negative and  $P$  has positive sign.

A three-curve model based on William-Warnke Criterion [15] is used to analyze the deviatoric stress tensor, as shown in figure 2, where the upper curve represents the maximum strength curve, the middle curve is the initial yield strength curve and the lower curve is the failed material residual strength curve [13].

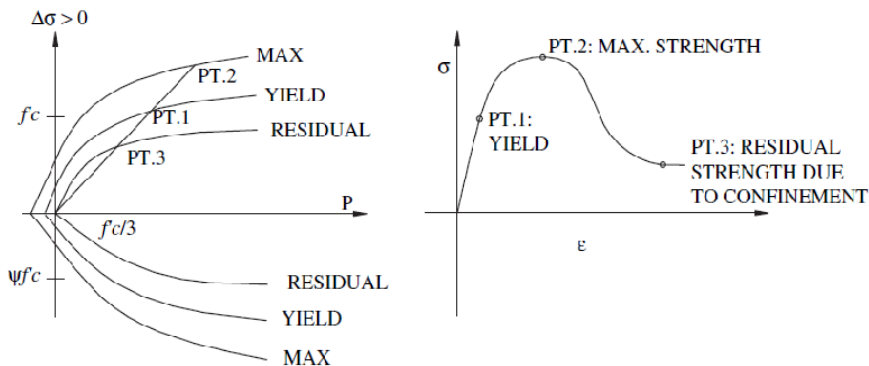


Figure 2: failure criteria for concrete [14]: (left) failure surfaces; (right) concrete constitutive model.

In order to consider the fact that under higher loading rates concrete and steel material exhibit increased strength, dynamic increase factors (DIF), the ratio of the dynamic to static strength, are employed in this analysis for Compressive and tension strength of the concrete and yield strength of the steel material. The expression proposed in CEB-fib (2010) is utilized for the concrete compressive strength as [16]:

$$DIF = \begin{cases} \left(\dot{\varepsilon}_c / 30 \times 10^{-6}\right)^{0.014} & ; \dot{\varepsilon}_c \leq 30s^{-1} \\ 0.012 \left(\dot{\varepsilon}_c / 30 \times 10^{-6}\right)^{1/3} & ; \dot{\varepsilon}_c > 30s^{-1} \end{cases} \tag{8}$$

Where  $\dot{\varepsilon}_c$  is the compressive strain rate. The DIF for concrete in tension is based on Malvar and Crawford (1998) [17] proposed equation as:

$$\text{DIF} = \begin{cases} \left( \frac{\dot{\epsilon}_{ct}}{10^{-6}} \right)^{\delta} & ; \quad \dot{\epsilon}_{ct} \leq 1 \text{ s}^{-1} \\ \beta \left( \frac{\dot{\epsilon}_{ct}}{10^{-6}} \right)^{1/3} & ; \quad \dot{\epsilon}_{ct} > 1 \text{ s}^{-1} \end{cases} \quad (9)$$

Where  $\dot{\epsilon}_{ct}$  is the tension strain rate in the range of  $10^{-6}$  to  $160 \text{ s}^{-1}$  and  $\beta = 10^{6\delta-2}$ ,  $\delta = \frac{1}{1+8\sqrt[4]{10}}$ . At any given pressure, the failure surfaces are expanded by a DIF which depends on the effective deviatoric strain rate.

The element erosion is the limit of eroded elements in material models in LS-DYNA. In this study, elements are eroded when their principle tensile strains reach 10 percent. In such case, separation of the eroded solid element from the rest of the mesh is occurred.

## 2.2 Steel material model

Steel is modelled as an elasto-plastic material with linear isotropic hardening that accounts for its strain rate effects. For the strain rate sensitivity, the expressions proposed by Cowper -Symonds [18] is utilized for yield stress of reinforcement as:

$$\text{DIF} = 1 + \left( \frac{\dot{\epsilon}_s}{40.4} \right)^{1/5} \quad (10)$$

Where  $\dot{\epsilon}_s$  is strain rate in the steel element. For steel material, erosion is occurred when the principle tensile strains reach 20 percent.

## 3. Verification of FEM

Verification of the finite element models as outlined in the above procedure is carried out by performing the analysis of a model under blast loading and comparing the results with an experimental research by Wu et al (2011) [6]. Experiment specimen is a column that was included with a top head and a foundation. The RC column specimen was designed based on the specifications provided by standard design codes and geometrically scaled down by two-thirds of the size of the column in a typical twenty-story residential building in Singapore. Column specimen has a cross-sectional dimension of  $400 \times 400 \text{ mm}$  and a vertical height of  $2400 \text{ mm}$ . The column specimen had a longitudinal reinforcement of eight T20 bars (nominal yield strength of  $420 \text{ MPa}$ ) and transverse reinforcement of R6 bars (nominal yield strength of  $280 \text{ MPa}$ ) placed  $125 \text{ mm}$  apart. Concrete with a characteristic compressive strength of  $30 \text{ MPa}$  was used to cast the specimen. The test was conducted by placing a charge, equivalent to  $25 \text{ kg}$  of TNT above the column specimen at stand-off distances of  $200 \text{ mm}$  from the face of the column. The specimen was placed horizontally. The TNT was placed on specimen at a distance of  $900 \text{ mm}$  measured along the column axial direction from its foundation. No column axial load was applied in the test. Details of the specimen and test setup are shown in figure 3.



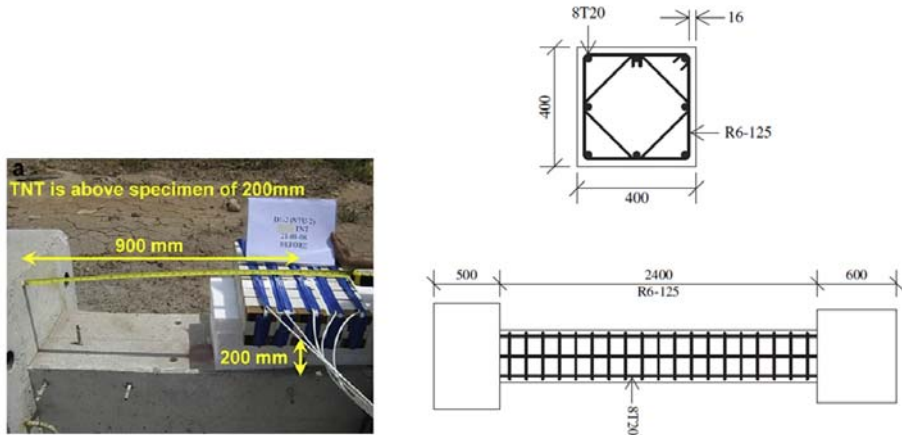


Figure 3: Geometry and section details of RC column specimen and test setup configuration [6].

Here, nonlinear dynamic analysis is done in the time domain by LS-DYNA explicit solver. It should be noted that concrete heads at both ends of the column are ignored and ideal simple and roller support conditions are defined at the ends. In a contact or near-field blast loading, extremely high peak overpressure is generated. The equipment utilized to measure the response history of the specimen fails when it is subjected to such high pressure. Thus the test results only provide damage profiles such as erosion zone of concrete and deformed shape of the specimen. Figure 4 shows the FE modeling and meshing of the considered column.

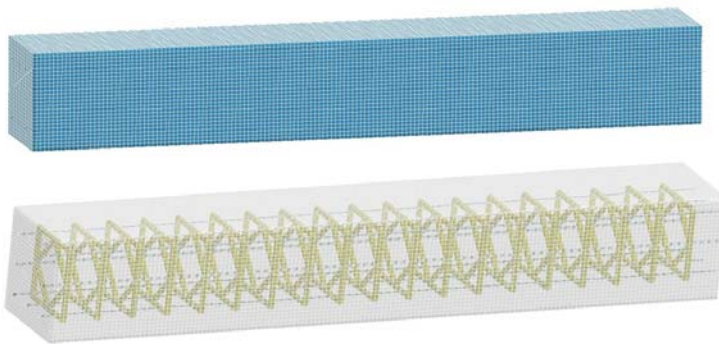


Figure 4: Finite element model of RC column specimen.

Figure 5 (left) shows a photograph of RC column specimen after being subjected to the explosive test. The analytical result for RC column specimen is shown in figure 5 (right) in which colors on the fringe plot indicate the contours of effective plastic strain. It is evident that the concrete erosion zone is 1200 mm in length. The analytical crack profile is very similar to the cracks sustained by the specimen from the actual charge, indicating that the numerical simulation produced fairly accurate results.

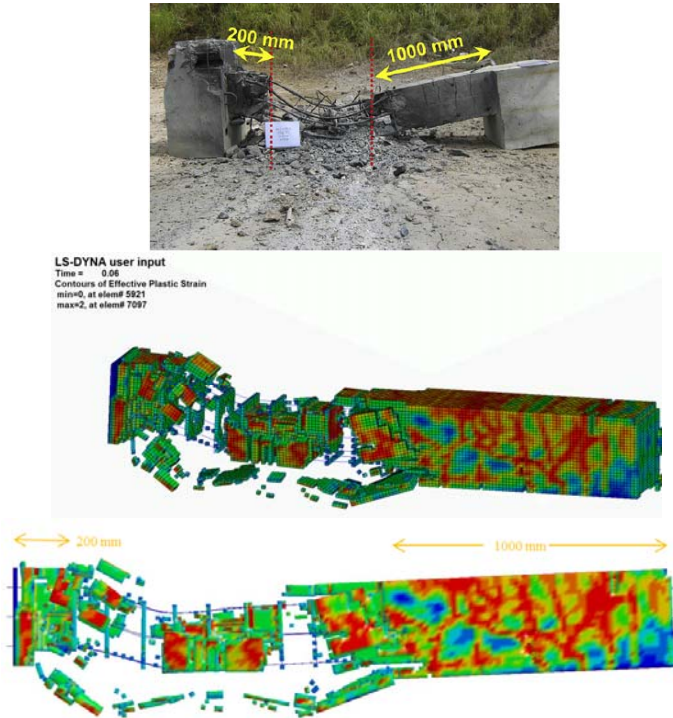


Figure 5: RC column specimen under explosive test and analytical results.

#### 4. Numerical Simulation Results

Using the finite element models discussed above, numerical simulations are performed to evaluate the dynamic response of RC columns under blast loading, and to estimate the residual axial capacity of the damaged columns. The behavior of columns subjected to blast conditions will be influenced their service gravity loads prior to being exposed to blast effects. Therefore, in the first loading stage, gravity load is applied via slow ramps to the column, while in the second loading stage, blast loads are applied dynamically and gravity load is remained fixed, simultaneously. Blast loads are calculated by LBE and are applied over the front face of the column and dynamic analysis is carried out. Eventually, in the post-blast loading stage, axial load is increased until the column is collapsed so residual capacity index can be determined. Here, collapse stage is defined as a state in which with 1% increasing in the axial load, displacement increases 10 %. This axial force must be applied gradually in an explicit dynamic analysis.

In this section, TNT explosive is used and located at a height of 1.5 m from the footing of columns. The explosive mass is  $W=10, 25$  and  $40$  kg with two different standoff distances  $R=0.5$  and  $3$  m. Hence, blast loading is performed with three different scaled distances of  $Z=0.23, 0.87, 1.0$  m/kg<sup>1/3</sup>. Mostly, we can assume the gravity load ratio  $P_L/P_{max}$  to be in the range of 0.1-0.4 [4,6].  $P_{max}$  easily may be calculated using equation below [19]:

$$P_{max} = 0.85f'_c(A_g - A_{sT}) + f_y A_{sT} \tag{11}$$

Where,  $A_{sT}$  is longitudinal reinforcement area and  $f_y$  is yield stress of the steel material. In this study,  $P_L/P_{max}$  ratios are assumed to be 0, 0.2 and 0.4.

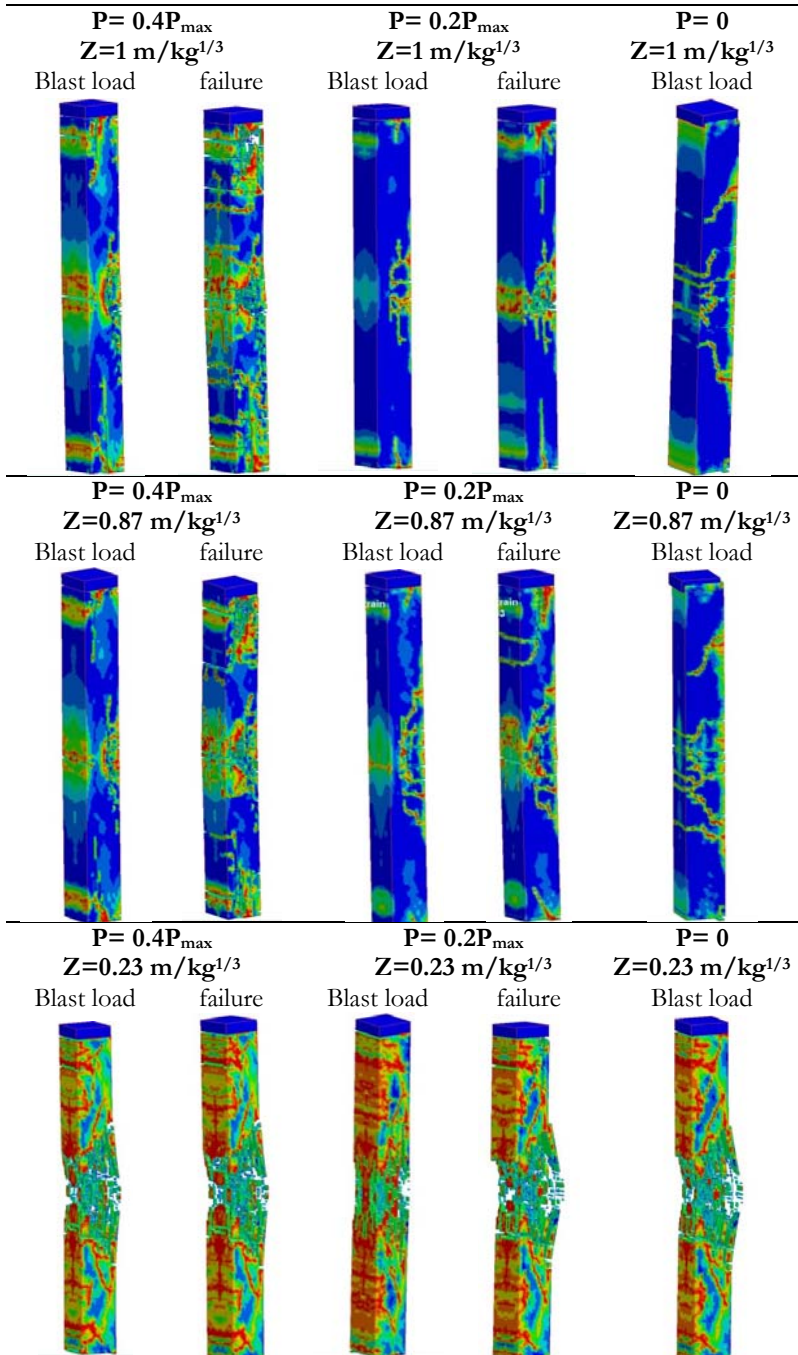


Figure 6: effective plastic strain contours under blast loads and near the axial failure.

In the figure 6 effective plastic strain contours after blast loading and near the axial failure state are shown. It can be seen that under axial load of  $0.2P_{max}$  deformation of the columns under blast loading is milder than the columns without axial force. With increasing the axial force to  $0.4P_{max}$  due to the secondary moment effects deformation of the column is increased. When there is no initial axial load in the column under the effect of blast loading with  $Z=0.87, 1 \text{ m/kg}^{1/3}$  scaled distance, shear failure at the top end of the column is observed. This event has caused to dramatic decrease in the axial load carrying capacity of the column. Subjected to blast loading with  $Z=0.23 \text{ m/kg}^{1/3}$  scaled distance, severe pressure is imposed to the column's face. Hence, the damage level to the column is very high.

Axial load time histories in the columns are shown in the figure 7. In these curves time is recorded after reaching blast wave to the structure. It is noted that in the blast loading stage, due to the inertia effect, the axial load supported by the column is not constant.

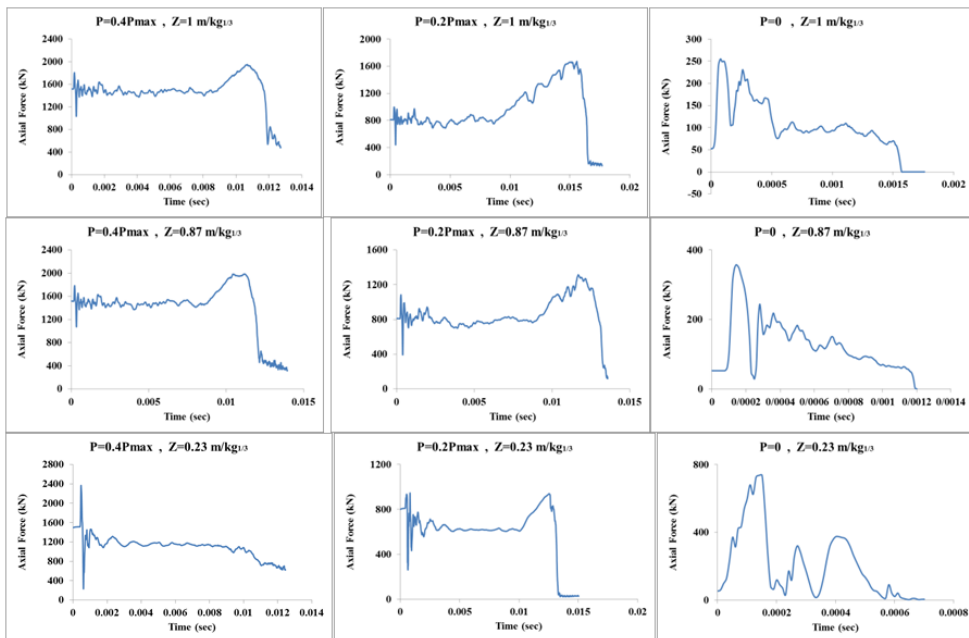


Figure 7: axial force verses time in the RC columns.

A summary of analysis results for residual axial capacity  $P_r$  and damage index  $D$  of the RC columns are indicated in the table 2. Estimated residual capacities resulted from empirical equations are listed, as well. According to the results, Wu et al (2010) and Arlery et al (2013) formulas were applicable only for three of the models considered here ( $Z=0.23 \text{ m/kg}^{1/3}$ ) because parameters in these relations  $\omega_{TNT}$  and  $R/d$  have limited domain. Hence, it is not possible to use these formulas for an extended range of blast loading scenarios.

**Table 2:** Estimation of residual axial load capacity of the RC columns.

No.	model	FEM		Bao and Li (2010)	Arlery et al (2013)	Wu et al (2010)			
		D	$P_r$ (kN)	$P_r$ (kN)	Diff. (%)	$P_r$ (kN)	Diff. (%)	$P_r$ (kN)	Diff. (%)
1	$P=0.4P_{max}$ $Z=1 \text{ m/kg}^{1/3}$	0.515	1940	2037	5	-	-	-	
2	$P=0.2P_{max}$ $Z=1 \text{ m/kg}^{1/3}$	0.582	1670	1475	11.7	-	-	-	
3	$P=0$ $Z=1 \text{ m/kg}^{1/3}$	1	0	880	-	-	-	-	
4	$P=0.4P_{max}$ $Z=0.87 \text{ m/kg}^{1/3}$	0.537	1850	1695	8.4	-	-	-	
5	$P=0.2P_{max}$ $Z=0.87 \text{ m/kg}^{1/3}$	0.672	1310	1500	14.5	-	-	-	
6	$P=0$ $Z=0.87 \text{ m/kg}^{1/3}$	1	0	880	-	-	-	-	
7	$P=0.4P_{max}$ $Z=0.23 \text{ m/kg}^{1/3}$	0.751	997	1355	35.9	1108	11.1	2339	-
8	$P=0.2P_{max}$ $Z=0.23 \text{ m/kg}^{1/3}$	0.765	940	1178	25.3	1108	17.9	2232	-
9	$P=0$ $Z=0.23 \text{ m/kg}^{1/3}$	1	0	880	-	1108	-	2108	-

Equation proposed by Wu et al (2010) takes in to account charge weight  $W$  (without standoff distance) and in the equation proposed by Arlery et al (2013) axial load effect is ignored. These are some reasons of differences between the results of FEM and estimated values by these two equations. In the case of column with high axial force level ( $P=0.4P_{max}$ ), Arlery et al (2013) has estimated residual strength that is 11.1% more than FEM result. For the case of lower axial force ( $P=0.2P_{max}$ ) this difference is 17.9%. The differences between FEM results for  $P_r$  are very far from Wu et al (2010) estimations. So, there must be done more investigations on this equation with other RC column models and loading conditions.

According to the table 2, equation proposed by Bao and Li (2010) has the closest predictions to FE analysis by LS-DYNA. Under the far field blast loading ( $Z=1, 0.87 \text{ m/kg}^{1/3}$ ), results of FEM and formula are more close together especially for upper axial load level ( $P=0.4P_{max}$ ). When the scaled distance is low ( $Z=0.23 \text{ m/kg}^{1/3}$ ) difference between analytical results and empirical formula is higher. For instance, under  $P=0.4P_{max}$  and  $Z=0.23 \text{ m/kg}^{1/3}$  the difference is 35.9%. Nonetheless, for the case of negligible axial force, this equation never predicts zero residual capacity but it is likely for a column without axial load to lose its axial strength under severe blast loading.

## 5. Conclusions

This paper is concerned with residual axial load carrying capacity of reinforced concrete columns after blast loading. Considered RC columns with square cross section are explicitly analyzed using LS-DYNA finite element software. As well, three empirical equations for estimating residual axial strength of RC columns are used and then the results of FEM are compared to empirical formulas calculations. Based on the main

results, equation proposed by Bao and Li (2010) has the closest predictions to FE analysis results under the far field blast loading ( $Z=1$ ,  $0.87 \text{ m/kg}^{1/3}$ ) especially for upper axial load levels ( $P= 0.4P_{max}$ ). Nonetheless, for the case of negligible initial axial force, this equation needs to be more investigated. Empirical equations proposed by Wu et al (2010) and Arlery et al (2013) have limited use and it is not possible to use these formulas for an extended range of blast loading scenarios. In the case of column with high axial force level ( $P= 0.4P_{max}$ ), Arlery et al (2013) equation has estimated residual strength close to FEM results. The differences between FEM results are very far from Wu et al (2010) estimations. So, there must be done more investigations on this equation with other RC column models and loading conditions.

## References

- Arlery, M., Rouquand, A., Chhim, S. (2013). Numerical Dynamic Simulations for the Prediction of Damage and Loss of Capacity of RC Column Subjected to Contact Detonations. In: 8<sup>th</sup> International Conference on Fracture Mechanics of Concrete and Concrete Structures (FraMCoS-8), Toledo.
- Shi, Y., Hao, H., Li, Z.X. (2008). Numerical Derivation of Pressure-Impulse Diagrams for Prediction of RC Column Damage to Blast Load. *International Journal of Impact Engineering*, 35(1):1213-27.
- Li, B., Nair, A., Kai, Q.A.M. (2012). Residual Axial Capacity of Reinforced Concrete Columns with Simulated Blast Damage. *Journal of Performance of Constructed Facilities*, 26(3): 287-299.
- Bao, X., Li, B. (2010). Residual strength of blast damaged reinforced concrete columns. *International Journal of Impact Engineering*, 37: 295–308.
- Tasai, A. (1999). Residual Axial Capacity and Restorability of Reinforced Concrete Columns Damaged Due to Earthquake. Technical report, Pacific Earthquake Engineering Research Centre (PEER) 10: 191–202.
- Wu, K.C., Li, B., Tsai, K.C. (2011). Residual Axial Compression Capacity of Localized Blast-Damaged RC Columns. *International Journal of Impact Engineering*, 38(1): 29-40.
- LSTC. (2015). *LS-DYNA Keyword User's Manual, Volume 1*. California: Livermore Software Technology Corporation.
- LSTC. (2015). *LS-DYNA Theory Manual*. California: Livermore Software Technology Corporation.
- LSTC. (2015). *LS-DYNA Keyword User's Manual, Volume 2: Material Models*. California: Livermore Software Technology Corporation.
- Krebs, J., Ho, P. (2012). Introduction to LS-PrePost 3.2. Livermore Software Technology Corporation Workshop.
- LS-DYNA support, Livemore. (2015). <<http://www.dynasupport.com/manuals/additional/lis-pre-post-v3.2-manual/view>>.
- Hong Tan, S., Koon Poon, J., Chan, R., Chng, D. (2012). Retrofitting of Reinforced Concrete Beam-Column via Steel Jachets against Close-in Detonation. In: 12th International LS-DYNA Users Conference, Michigan.
- Schwer, L., Malvar, L.J. (2005). Simplified Concrete Modeling with MAT\_CONCRETE\_DAMAGE\_REL3. JRI LS-Dyna User Week, Nagoya.
- Malvar, L.J., Crawford, J.E., Wesevich, J.W., Simons, D. (1997). A Plasticity Concrete Material Model for DYNA3D. *International Journal of Impact Engineering*, 19.9: 847–73.
- Chen, W.F. (2007). *Plasticity in Reinforced Concrete*. New York: J ROSS.
- Federal Institute of Technology. (2010). *Model Code 2010, First Complete Draft, Volume 1: fib Bulletin 55*. Switzerland: fib.
- Malvar, L.J., Crawford, J.E. (1998). Dynamic Increase Factors for Concrete. In: 28<sup>th</sup> DDESB Seminar, Orlando.
- Cowper, G.R., Symonds, P.S. (1958). Strain Hardening and Strain Rate Effects in the Impact Loading of Cantilever Beams. Brown University, Applied Mathematics Report.
- ACI 318 Committee. (2011). *Building code requirements for structural concrete and Commentary (318-11)*. Farmington Hills: American Concrete Institute.